Analyst

RSC Publishing

PAPER

View Article Online
View Journal | View Issue

Cite this: *Analyst*, 2013, **138**, 2576

Highly sensitive grating coupler-based surface plasmon-coupled emission (SPCE) biosensor for immunoassay

Jong Seol Yuk,[a] Ernest F. Guignon[b] and Michael A. Lynes*[a]

Received 18th January 2013
Accepted 7th March 2013

DOI: 10.1039/c3an00135k

www.rsc.org/analyst

We have evaluated the performance of a novel high-content gold grating coupler-based surface plasmon-coupled emission (SPCE) biosensor system. The polyelectrolyte (PEL) layer on the system's biosensor chip surface was formed on the gold surface using a layer-by-layer (LbL) deposition technique to spatially separate fluorophores from the gold surface and as a linker layer for protein immobilization. The characteristics of the PEL spacer layers were determined by surface plasmon resonance (SPR) analysis and by ellipsometry. The SPCE response decreased as the spacer layer thickness increased above a dominant quenching range (10 nm). Two PEL layers of poly(diallyldimethylammonium chloride) and poly(acrylic acid) were found to be an effective spacer that minimized the quenching effect while maximizing SPCE responses for both direct and sandwich immunoassay formats. A mouse IgG sandwich immunoassay using this optimized spacer layer configuration showed a dose-dependent response with a 1 pg ml^{-1} limit of detection by the 3σ rule. A nine log dynamic range of human IgG concentrations in unfractionated human serum could be analyzed using this approach. These results show the potential of the grating coupler-based SPCE biosensor as a sensitive platform for high-content analysis.

1 Introduction

Measurements of surface plasmon-coupled emissions (SPCE) have emerged as a novel biosensing technology for analysis of biomolecular interactions[1,2] on protein arrays. There are several unique characteristics that distinguish SPCE from surface plasmon resonance (SPR).[3,4] SPCE optical biosensors are highly sensitive because this technology can significantly improve fluorescence collection efficiency while suppressing background bulk fluorescence from the solution due to the near-field interaction.[1]

Protein arrays have become a promising tool for various biological applications such as measurements of protein–protein and DNA–protein interactions, protein expression profiling, drug screening and biomedical diagnostics.[5,6] Protein arrays allow scientists and clinicians to study large sets of proteins simultaneously in a rapid, low-cost and low sample volume format.[7,8] There are a number of advantages to analyzing biological processes at the protein level using SPCE. For example, SPCE can be used to assess dynamic changes in protein concentration. Since mRNA levels do not always correlate with protein abundance, results from oligonucleotide arrays that are used to suggest protein abundance can be misleading in some circumstances.[9] A number of technologies have been used in the analysis of protein arrays including enzyme-linked immunosorbent assay (ELISA), isotropic labeling, non-contact atomic force microscopy, planar waveguides, surface-enhanced laser desorption/ionization mass spectrometry, surface plasmon resonance (SPR)[10,11] and paraboloid element geometry-based SPCE.[12] Even though the three-dimensional paraboloid element enables collection of fluorescence with high efficiency, the paraboloid element geometry-based SPCE biosensor is limited by the number of paraboloid elements that can be for used high-content analysis because it is difficult to reduce paraboloid element size to sub-mm scale for placement on a gold sensor film. Grating coupler-based SPCE overcomes this limitation because the grating coupler-based sensor chip is capable of measuring more than 1000 spatially encoded regions of interest on a 1 cm^2 holographic diffraction grating.[13]

One of the potential limitations associated with highly sensitive SPCE measurements is a quenching effect caused by radiationless resonance energy transfer to the gold surface. For most sensor chips, gold is the preferred sensor chip surface material because gold has better long-term chemical stability than silver or other SPR-active metals in an aqueous environment. However, gold is also a strong quencher for fluorophores placed within close proximity to the gold surface.[14] In most SPCE experiments, materials such as Langmuir–Blodgett films or SiO_2 have been used as a spacer layer to minimize these metal quenching effects.[15–18]

In this work, we demonstrate gold grating coupler-based SPCE responses on an optimized spacer layer composed of

[a]*Department of Molecular and Cell Biology, University of Connecticut, 91 North Eagleville Road, Storrs, CT 06269-3125, USA. E-mail: michael.lynes@uconn.edu; Fax: +1-860-486-4331; Tel: +1-860-486-4350*

[b]*Ciencia Inc., East Hartford, CT, USA*

polyelectrolyte (PEL) layers and protein layers. The PEL layer was used not only to minimize the quenching effects, but also to facilitate the capture protein's attachment to the sensor chip surface.[19] The PEL-based layers were prepared using an established layer-by-layer (LbL) deposition technique that relies on electrostatic interactions.[20] The manipulations of layer thickness were confirmed by both SPR analysis and ellipsometry. The sensitivity of the SPCE responses on an optimized spacer layer for the direct and sandwich assay formats were compared with that of ELISA measurements of the same molecular interactions. Using this approach, the gold grating coupler-based SPCE biosensor had a limit of detection (LOD) of 1 pg ml^{-1} mouse IgG in buffer solution and 34 pg ml^{-1} human IgG in unfractionated human serum.

2 Experimental

2.1 Chemicals and reagents

11-Mercaptoundecanoic acid (MUA), cysteamine, poly(diallyldimethylammonium chloride) (PDDA) ($M_w \sim 100\,000$), poly(sodium 4-styrenesulfonate) (PSS) ($M_w \sim 70\,000$) and poly(acrylic acid) (PAA) ($M_w \sim 100\,000$) were purchased from Sigma (St. Louis, MO). *N*-Ethyl-*N*′-(dimethylaminopropyl)-carbodiimide (EDC) and *N*-hydroxysuccinimide (NHS) were purchased from Pierce (Rockford, IL). Mouse IgG and goat anti-mouse IgG (H + L chain specific) were from Upstate Biotechnology (Lake Placid, NY) and bovine serum albumin (BSA) was from Sigma (St. Louis, MO). Human IgG and goat anti-human IgG (H + L chain specific) were from Fisher Scientific Inc. (Pittsburgh, PA). Alexa Fluor 647-goat anti-mouse IgG, Alexa Fluor 647-goat anti-human IgG and human serum were purchased from Invitrogen (Carlsbad, CA). All other chemical reagents were of analytical grade.

2.2 SPCE instrumentation

An optical schematic of the grating-based dual mode SPR/SPCE chip reader (Ciencia, Inc., East Hartford, CT) is shown in Fig. 1C. A 635 nm laser diode was used as a light source and a polarizer was positioned in the input path of the light to make *p*-polarized light. Images of the sensor chip are taken over a range of angles to obtain the SPR signal. Twelve bit grey scale bitmap images (1392 × 1040 pixels) from the CCD camera are stored and processed in the linked computer. Calculated SPCE intensities for quantitative analysis represent average values at each region of interest. The summation of the intensity of each pixel is divided by the number of pixels in the region of interest. The field of view of the CCD camera is approximately 13 × 13 mm^2 and the resolution of the image is estimated to be 19 × 25 μm^2. Motion control, data acquisition, image processing, and display are accomplished using LabVIEW-based software.

2.3 Sensor chip

Dual mode sensor chips with 500 nm pitch were purchased from Ciencia Inc. (East Hartford, CT). The sensor chips were washed with 100% ethanol and rinsed with distilled water to remove any surface contamination. The SpotBot® 2 microarrayer (Arrayit Corporation, Sunnyvale, CA) was used to deposit proteins on the sensor chip surface, ArrayIt Stealth micro spotting SMP7B pin (3.1 nl delivery volume with 255 μm spot diameter and spotting density of 1024 spot per cm^2).

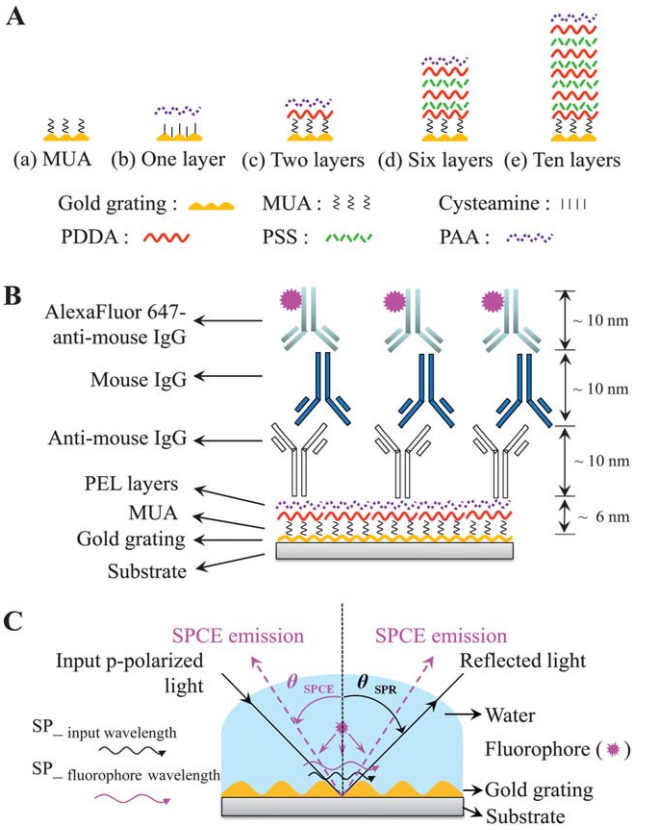

Fig. 1 Surface structure of sensor chips and schematic diagram of grating coupler-based SPCE. (A) Gold surfaces were modified with MUA (a), PAA (b), PDDA/PPA (c), [PDDA/PSS] × 2/PDDA/PAA (d), and [PDDA/PSS] × 4/PDDA/PAA (e) on the self-assembled monolayer of cysteamine or MUA. (B) Surface structure of mouse IgG sandwich immunoassay on the sensor chip. Protein layer geometry was based on the size of IgG (Y-shape, height = 14.5 nm, width = 8.5 nm, thickness = 4.0 nm).[28] (C) Highly directional SPCE is produced with the near-field interaction between fluorophores and the gold surface. Two surface plasmons (SPs) are involved in the SPCE.

2.4 Surface modification of sensor chips with polyelectrolytes

In most experiments, the spacer polyelectrolyte layer was deposited using the LbL technique. Fig. 1A shows the multilayer polyelectrolyte surfaces prepared by the LbL technique, whose surfaces were alternately coated with two oppositely charged polyelectrolytes. Briefly, gold surfaces were incubated with 10 mM MUA in ethanol for 30 min, resulting in the formation of a self-assembled monolayer of MUA.[21] After rinsing with 100% ethanol, the surfaces were treated with 0.05 N NaOH for 5 min. Then, charged array surfaces were prepared by alternating incubation for 10 min with 2 mg ml^{-1} PDDA (positively charged) and 2 mg ml^{-1} PSS (negatively charged) in 0.1 M NaCl. After two or four alternating incubations with PDDA and PSS, the surfaces

were washed with deionized H_2O (18 MΩ) and PDDA was incubated on the PSS surface to produce a final positively charged surface. These positively charged surfaces were incubated with 2 mg ml^{-1} PAA before final modification with individually spotted capture proteins.

2.5 Preparation of sensor chips for a sandwich assay

To facilitate capture protein binding, the carboxyl group of PAA was activated to form reactive *N*-hydroxysuccinimide esters using a solution of 50 mM *N*-hydroxysuccinimide and 200 mM *N*-ethyl-*N*′-(dimethylaminopropyl)-carbodiimide in water for 10 min. The capture protein, goat anti-mouse IgG; (400 μg ml^{-1} in 10 mM acetate buffer, pH 4.5), was then immobilized on the polyelectrolyte surface for 24 h at 4 °C in a humid chamber. The sensor chip was washed with 0.1% Tween 20 in phosphate-buffered saline (PBS) (8.1 mM Na_2HPO_4, 1.2 mM KH_2PO_4, 138 mM NaCl, 2.7 mM KCl, pH 7.4) for 10 min, and rinsed with deionized H_2O (18 MΩ) and briefly dried under a stream of air. Blocking to reduce subsequent non-specific binding was then performed by incubating the sensor chip surface with a blocking solution (3% BSA in the PBS contained 0.1% Tween 20, pH 7.4) for 1 h at room temperature in a humid chamber. The sensor chip was next washed with 0.1% Tween 20 in PBS for 10 min, and rinsed with deionized H_2O. Various concentrations of mouse IgG (1 pg ml^{-1} to 100 μg ml^{-1}) were prepared by dilution with 0.1% BSA in PBS containing 33% glycerol. Protein solutions of mouse IgG were printed to the sensor chip surface with the SpotBot II robotic spotter. The sensor chip was incubated for 3 h at room temperature and washed as described above. Alex Fluor 647 labeled goat anti-mouse IgG (200 μg ml^{-1}) prepared with 0.1% BSA in the PBS contained 0.1% Tween 20 was next applied to the chip in bulk solution and incubated for 1 h. After incubation, the sensor chip was washed with 0.1% Tween 20 in PBS for 10 min, rinsed with deionized H_2O and analyzed by the dual mode sensor chip reader.

2.6 Preparation of sensor chips for analysis of human serum

For analysis of human serum, goat anti-human IgG (400 μg ml^{-1}) was immobilized on the chip by covalent binding, and incubated with blocking solution for 1 h at room temperature in a humid chamber as described above. Human serum was diluted 1 : 10 to 1 : 10^9 with 0.1% BSA in PBS (pH 7.4) containing 33% glycerol, and these dilutions were individually printed to specific region of interests (ROIs) on the anti-human IgG immobilized sensor chip surface with the SpotBot II robotic spotter after washing the sensor chip. Human serum-printed chips were incubated for 3 h at room temperature and washed as described above. After washing, Alexa Fluor 647-labeled anti-human IgG (200 μg ml^{-1}) diluted with 0.1% BSA in the PBS contained 0.1% Tween 20 was next applied to the chip surface in bulk and incubated for 1 h in a humid chamber. After incubation, the chip was washed with 0.1% Tween 20 in PBS for 10 min, and rinsed with deionized H_2O before analysis in the SPCE reader.

2.7 Enzyme-linked immunosorbent assay (ELISA)

Wells of a 96-well Immulon 2 HB microplate (Thermo Labsystems, Hudson, NH) were filled, in triplicate, with 100 μl of 4 μg ml^{-1} goat anti-mouse IgG in PBS and incubated at 4 °C for 24 h. Wells were then washed three times with buffer (0.1% Tween 20 in PBS) using an ELX405 automated washer (Biotek Instruments, Winooski, VT) and then blocked with 200 μl of 2% BSA in PBS at 37 °C for 1 h. Various concentrations of mouse IgG (0.0001–10 μg ml^{-1}) were prepared in blocking buffer. The prepared mouse IgG solutions were added to appropriate wells, incubated at 37 °C for 1 h, and washed as before. Antibody–enzyme conjugate (100 μl) was then added to each well, incubated at 37 °C for 1 h, and washed. Finally, 100 μl substrate buffer (9.7 ml of diethylamine, 80 ml distilled H_2O, 0.02 g of NaN_3, 0.01 g of $MgCl_2 \cdot 6H_2O$) with 10 mg *para*-nitrophenylphosphate (PNPP)/10 ml buffer was added to each well. Changes in optical density at 405 nm over 10 minutes were measured using an SPECTRAmax M2 microplate reader (Molecular Devices, Downingtown, PA) in kinetic mode, and plotted as mOD min^{-1}.

3 Results and discussion

3.1 Immobilization of proteins on the PAA surface

Proteins may undergo denaturation when immobilized on solid substrates such as glass or gold, hence it is important to minimize denaturation during surface modification.[22] We investigated whether the polyelectrolyte PAA could be used as a covalent binding surface to immobilize antibody with minimal denaturation. Sensor chips were incubated with 10 mM cysteamine for 30 min to make a self-assembled monolayer on the gold surface, and were then treated with 0.05 N HCl for 5 min to produce a positively charged surface. The PAA was immobilized on the cysteamine surface by electrostatic interaction between positively charged cysteamine and negatively charged PAA. Alexa Fluor 647-labeled anti-mouse IgG (100 μg ml^{-1}) was next immobilized on the PAA surface *via* covalent binding between the carboxyl group of PAA and amine groups of the antibody. Other sensor chips that had been modified with MUA were compared to the PAA modified chips, since immobilization of proteins on MUA has been previously demonstrated.[21] MUA is a bifunctional cross-linker with functional groups (SH) that react with the gold surface and carboxyl groups that interact with the protein. Alexa Fluor 647-labeled anti-mouse IgG (100 μg ml^{-1}) was immobilized on the MUA surface using covalent binding.[23] Fig. 2A shows SPCE images of the two sensor chips employing PAA and MUA modifications. The SPCE image on the PAA-modified chip was brighter than that on the MUA modified surface when imaged under the same conditions. For quantitative analysis, SPCE intensities were calculated from these images (Fig. 2B). The SPCE intensity suggests using the PAA surface modification improves sensitivity more than the MUA modification. An explanation for this observation is that the SPCE response on the MUA surface has been reduced due to the quenching effect that is related to the thickness of a spacer layer (the distance between the gold surface and the Alexa Fluor 647-fluorophore). The spacer layer formed

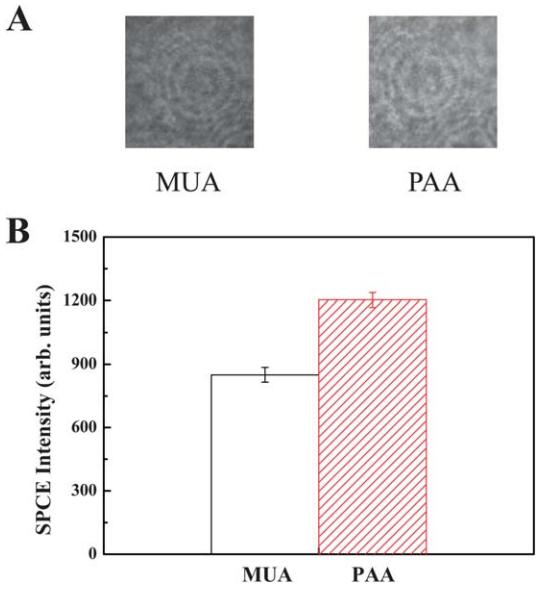

Fig. 2 Comparison of SPCE responses on MUA and PAA surfaces. (A) Representative SPCE images of Alex Fluor 647-labeled goat anti-mouse IgG (100 μg ml^{-1}) immobilized on MUA- and PAA-modified surfaces. (B) SPCE intensities were calculated from the SPCE images of (A).

with PAA is thicker than that of the monolayer MUA because PAA covers the gold surface as a polymer on the underlying cysteamine surface (Fig. 1A(a and b)).

3.2 Characterization of LbL films

To investigate the sensitivity of the SPCE response to spacer layer thickness, we used two different charged polyelectrolytes (PDDA and PSS) in order to vary spacer thickness. Two, six, and ten layers of the polyelectrolyte multilayer were made on the gold surface with the LbL technique by successive deposition employing electrostatic interactions between adjacent layers of opposite charge. To immobilize Alexa Fluor 647-labeled anti-mouse IgG to the final layer, PAA was deposited on the final positively charged PDDA surface.

We confirmed the incremental change in polyelectrolyte layer thickness using SPR image analysis. Fig. 3A shows SPR images of the sensor chips after Alexa Fluor 647-labeled antibody immobilization on 2, 6, and 10 polyelectrolyte layers, and the SPR images were acquired at the 7.7° angle of incidence (which was the SPR angle of the gold surface).[2] The SPR image becomes brighter at this angle with increasing polyelectrolyte layer thickness. To compare the experimental SPR response to a theoretical SPR calculation, the SPR reflectivity was calculated as a five-phase system (glass substrate/gold/polyelectrolyte/protein/water) with a diffraction grating solver based on the integral method for the 635 nm excitation wavelength.[24] Gold (50 nm) on the glass substrate ($n = 1.515$) was used for the SPR spectrum calculations.[25,26] The protein layer was assumed to be 10 nm thick with a refractive index of 1.45 (ref. 27 and 28) and the refractive index of polyelectrolyte layer was 1.53.[12] Fig. 3B shows that the SPR reflectivity curve shifted to higher angles of incidence and reflectivity at 7.7° increased as the polyelectrolyte

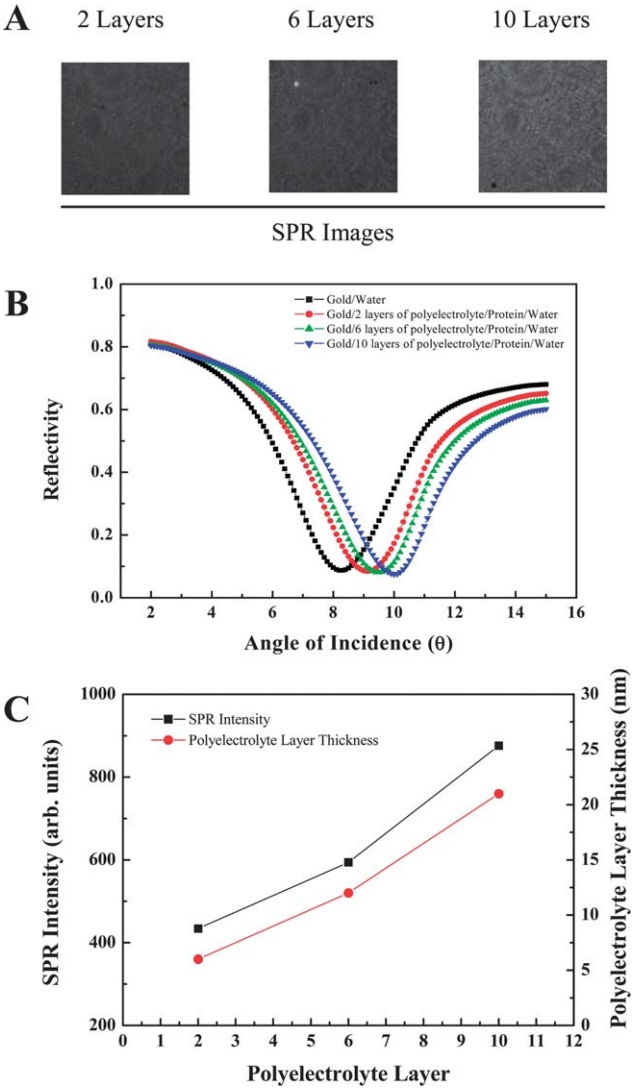

Fig. 3 Analysis of polyelectrolyte layers with SPR response. (A) Representative SPR images acquired on the various polyelectrolyte layers immobilized Alex Fluor 647 labeled goat anti-mouse IgG (100 μg ml^{-1}). (B) Reflectivity for a five-phase system with glass substrate/gold/polyelectrolyte/protein/water was calculated using a diffraction grating solver based on the integral method. The optical parameters used in the model were 50 nm gold and BK-7 glass substrate with refractive index of 1.515. The protein layer was assumed to be 10 nm ($n = 1.45$) and the polyelectrolyte layer refractive index used was 1.53. Calculated values are plotted for 3 different polyelectrolyte thicknesses. (C) SPR intensities were calculated from the SPR images of (A) for quantitative analysis. Thickness of the polyelectrolyte layers was measured with the ellipsometer L117F300.

layer thickness increased. SPR images were acquired from the intensity of the SPR reflectivity near the resonance angle of the gold surface.[29] The intensity of the SPR reflectivity is directly proportional to the SPR intensity calculated from the SPR image acquired at the resonance angle of the gold surface (Fig. 3C). Changes of the polyelectrolyte layer thickness could be confirmed using the SPR response since it has been shown that the SPR response changes in proportion to dielectric thickness.[30,31] The polyelectrolyte layer thickness was confirmed with a variable angle manual ellipsometer L117F300 (Gaertner Scientific Corporation, Skokie, IL).

Having measured changes in polyelectrolyte layer thickness by both SPR and ellipsometry, we next determined whether increasing the spacer layer thickness by including protein layers would influence the quenching effect on the gold grating coupler-based SPCE response. According to a report describing this quenching effect,[32] the lifetime of the excited state of fluorophores is dominated by radiationless resonance energy transfer to the metal surface when the fluorophore is separated from the metal by less than 10 nm. Excited fluorophores interact through the near-field with the metal surface, and excitation energy is dissipated as heat into the metal.[33] Gold is known to be a strong quencher of fluorophores placed in close proximity.[14] Normalized fluorescence intensity as a function of distance is plotted in Fig. 4, which was calculated as described in a previous report:[34]

$$I_d/I_\infty = [1 + (d_0/d)^4]^{-1}, \quad (1)$$

where I_∞ denotes the fluorescence intensity at infinite separation distance and I_d is the observed fluorescence intensity with the fluorescent dyes being separated at a distance d. d_0 is called the Förster radius and it is the distance at which half of the energy is transferred, and depends on the spectral characteristics of the dye and its orientation.[35] These results show that the fluorescence intensity increases linearly below 10 nm, where the fluorescence intensity is 81%. At greater distances (above 20 nm), the fluorescence reaches saturation. We calculated normalized electric field intensity of surface plasmons as a function of distance for the 635 nm excitation wavelength from the gold surface.[36] As shown in Fig. 4, the evanescent field of surface plasmons decreases with increasing distance from the gold surface.[37] The product of the two curves was calculated to find an optimum distance for the SPCE response. The theoretical result of this calculation in Fig. 4 indicates that the optimum distance of the fluorophore from the gold surface is approximately 15 nm. We predict that the SPCE response will be reduced at spacer thicknesses greater than 15 nm, even if the quenching effect is completely eliminated.

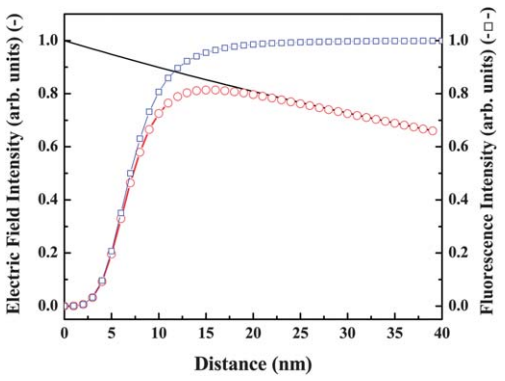

Fig. 4 Characteristics of electric field intensity and fluorescence intensity according to distance. Normalized electric field intensity of surface plasmons (–) was calculated as a function of distance from the gold surface. The surface plasmons were excited at the gold (50 nm)–water interface with 635 nm. Normalized fluorescence intensity (□) as the Förster energy transfer mechanism was calculated as a function of distance from the gold surface considering the Förster radius of 7 nm. The optimum separation distance between gold surface and fluorophore can be determined by the product of the two curves (○).

3.3 Optimum spacer layer of bioassay for SPCE response

To test these predictions, we measured SPCE responses using various spacer thicknesses that include the protein layers, as would be part of a real life bioassay. A spacer layer of SiO_2 has been used to reduce the quenching effect on the gold surface in other SPCE experiments. Protein layers can be also used as an anti-quencher layer in SPCE-based bioassays.[19]

In these experiments, the protein layers of mouse IgG and Alexa Fluor 647-labeled anti-mouse IgG were considered as part of the spacer layer[19] that included the polyelectrolyte surfaces. Similar to results shown in Fig. 4, the SPR image becomes brighter at a specific angle upon increasing the spacer layer (Fig. 5A). The SPR intensity in Fig. 5C is substantially higher than that of Fig. 3C at the same interrogation angle. From the SPR analysis, we interpret this data to indicate that the Alexa Fluor 647 dye was located at a greater distance from the metal surface compared to the experiments shown in Fig. 3. However,

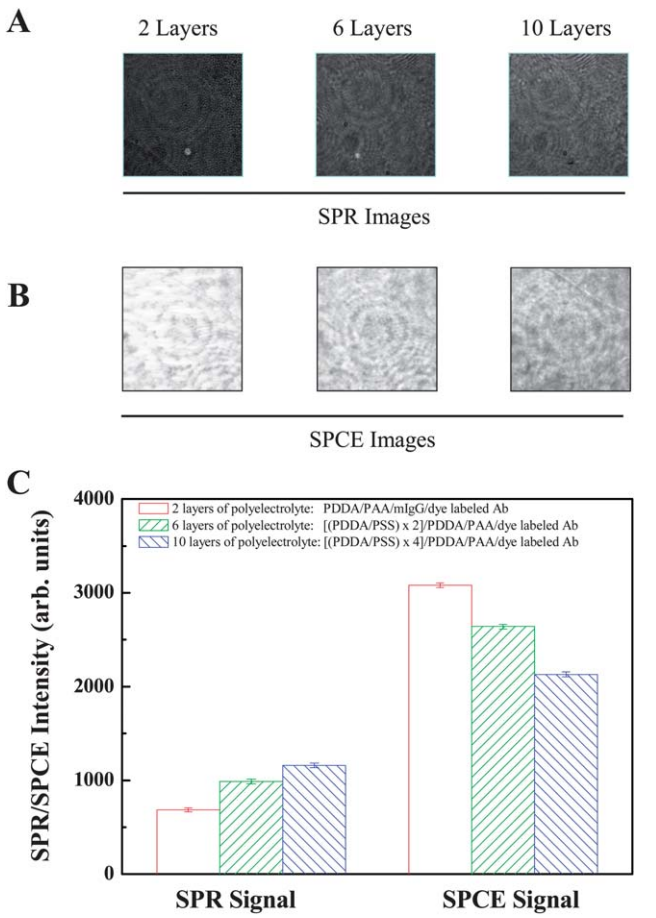

Fig. 5 Analysis of sensor chips on the various spacer layers included protein layers. (A) SPR and (B) SPCE images were acquired with the same sensor chips. Alex Fluor 647-labeled goat anti-mouse IgG (100 μg ml^{-1}) was incubated on the mouse IgG immobilized on the various polyelectrolyte spacer layers. (C) SPR and SPCE intensities are shown as a function of the spacer layer composition, including protein layers.

as shown in Fig. 5B, the SPCE image becomes darker with increasing spacer layer thickness. The quenching effect can be neglected because the normalized fluorescence intensity is saturated when the dye is located at a distance greater than 10 nm from the gold surface (Fig. 4). It is possible to explain the SPCE response as a reduction of the evanescent field intensity of surface plasmons. A strong evanescent field intensity of surface plasmons would excite more Alexa Fluor 647 than a weak field intensity because the evanescent field is decreased as the fluorophore is located at a greater distance from the gold surface. As a consequence, we conclude that two polyelectrolyte layers (PDDA/PAA) represent an optimum polyelectrolyte layer configuration for bioassay applications.

3.4 Mouse IgG immunoassay and serum analysis

Direct assays employ labeled primary antibodies that react directly with antigens that are immobilized on the sensor chip surface. For these experiments, various concentrations of mouse IgG were immobilized on the sensor chip surface (Fig. 6A). Sandwich assays use labeled secondary antibodies (detection antibodies) and are generally more sensitive and versatile. In this assay configuration, primary antibodies (capture antibodies) are immobilized on the sensor chip surface and react with antigens. The capture of the antigen is then detected with a labeled matched-pair antibody specific for a second epitope on the captured antigen. Various concentrations of mouse IgG (the antigen) were immobilized on the anti-mouse IgG (Fig. 6A), and detected with matched pair the Alexa Fluor 647-goat anti-mouse IgG.

Having optimized the dimensions of the polyelectrolyte layer for SPCE responses, an immunoassay for the analyte mouse IgG was carried out to determine the limit of detection (LOD) and dynamic range for this assay configuration. This direct assay used labeled primary antibodies that react directly with antigen that is immobilized on the sensor chip surface. As shown in Fig. 6A, SPCE intensity increases as the concentration of mouse IgG increases in both the sandwich and direct assays. The LOD of the sandwich assay, using the 3σ rule, was estimated to be 1 pg ml^{-1} for this specific antibody–antigen pair. This LOD of the SPCE response was compared with that of the direct assay on the same polyelectrolyte layer and that of an enzyme-linked immunosorbent assay (ELISA) using the same reagents to evaluate the SPCE performance. The LOD of the direct assay was estimated to be 10 pg ml^{-1} for the same specific antibody–antigen pair. The SPCE response level of the sandwich assay is higher than that of the direct assay using the same polyelectrolyte layer configuration. We hypothesize that this increased sensitivity in the sandwich assay results from the multiple binding sites of mouse IgG that can be bound by the labeled detection antibody. The LOD for antigen–antibody combination using an antibody conjugated to alkaline phosphatase for the matched pair reagent in ELISA is 100 pg ml^{-1} (Fig. 6A). There has been a report of IgG detection by ELISA with an LOD of 20 pg ml^{-1} in buffer by a 2σ criterion.[17] For comparison, electrochemical stripping detection is reported to have an LOD of 50 pg ml^{-1} for human IgG using copper-enhanced gold nanoparticle tags.[38] An SPCE biosensor that uses a combination of bimetallic films and a SAF-based paraboloid biochip for analysis of human IgG has recently been reported with an LOD of 1 pg ml^{-1}.[39] The current approach described here improves the sensitivity of the gold grating coupler-based SPCE biosensor simply by optimizing the effect of quenching and evanescent field intensity without the use of nanoparticles or specialized detection geometries, while maintaining a high content configuration.

We measured human IgG concentrations in complete human serum using this optimized configuration with the same sandwich assay protocol. In these experiments, dilutions of human serum (1 : 10 to 1 : 10^9) were spotted on a sensor surface treated with PAA and anti-human IgG. As shown in Fig. 6B, dose dependent responses were observed from the serial dilutions of human serum. We could detect human IgG in the highest dilution of human serum used (1 : 10^9) by SPCE. To determine the concentration of human IgG in the diluted sera, we performed ELISA experiments with known concentrations of human IgG in buffer solution to prepare a calibration curve (data not shown). Concentrations of IgG in human serum were estimated based on this calibration curve (data not shown). The lowest dilution factor (1 : 10^9) of human serum that produced a significant SPCE response corresponds to 34 pg ml^{-1} human IgG.

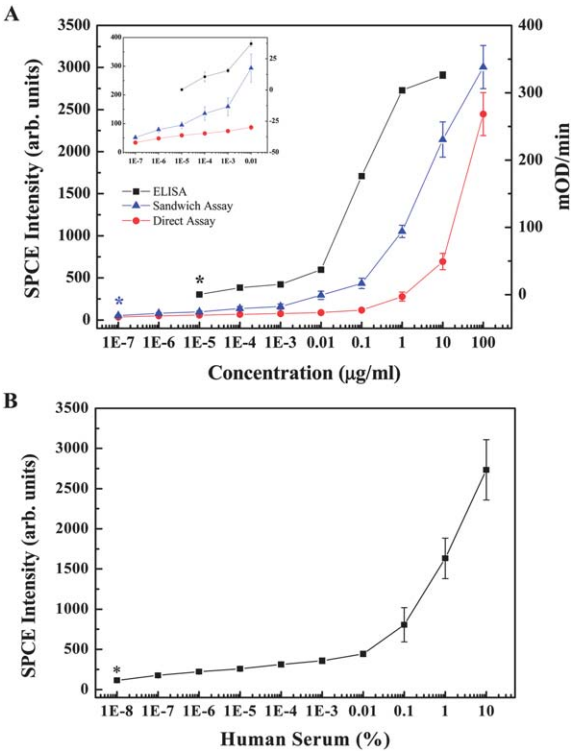

Fig. 6 Mouse IgG immunoassay and analysis of human IgG in human serum. (A) Various concentrations of mouse IgG were incubated on anti-mouse IgG immobilized on the PDDA/PAA polyelectrolyte layer. Sensitivity of SPCE in sandwich assay was compared with direct assay and ELISA. The values indicated by (*) were used as a reference to monitor signal changes. Insert figure has been enlarged between 1 pg ml^{-1} and 10 ng ml^{-1} values to show more detail for direct and sandwich SPCE assay. (B) Analysis of human IgG immunoassay in human serum.

4 Conclusion

We have demonstrated a highly sensitive gold grating-based SPCE biosensor that has been optimized by achieving a compromise between the quenching effect and the evanescent field intensity of surface plasmons. Polyelectrolyte spacer layers were formed on the gold grating surface with the LbL deposition technique, and confirmed with SPR analysis and ellipsometry. The quenching effect is reduced as the spacer layers increase in number. However, the SPCE response decreases when the spacer layer thickness is increased beyond the dominant quenching range (10 nm). In our bioassay experiments, two polyelectrolyte layers (PDDA/PAA) was the optimum number for increasing the SPCE response. One pg ml^{-1} LOD was achieved with the model mouse IgG immunoassay and 34 pg ml^{-1} human IgG could be detected in human serum indicating a minor matrix effect of the sample. This work suggests that the gold grating-based SPCE biosensor can be used as a very sensitive sensing platform with wide dynamic range for high-content analysis of biomolecular interactions.

Acknowledgements

This research was funded by grants for the National Institutes of Health (GM075407, A1066482, and ES016014). We thank James M. Rice and Clare Melchiorre for assistance with the research work and JMR for critical reading of the manuscript. We thank Robert A. Croce and Gaertner Scientific Corporation for assistance with ellipsometer measurements.

References

1 J. R. Lakowicz, K. Ray, M. Chowdhury, H. Szmacinski, Y. Fu, J. Zhang and K. Nowaczyk, *Analyst*, 2008, **133**, 1308.
2 J. S. Yuk, N. G. Gibson, J. M. Rice, E. F. Guignon and M. A. Lynes, *Analyst*, 2012, **137**, 2574.
3 J. S. Yuk, E. O'Reilly, R. J. Forster, B. D. MacCraith and C. McDonagh, *Chem. Phys. Lett.*, 2011, **513**, 112.
4 I. Gryczynski, J. Malicka, Z. Gryczynski and J. R. Lakowicz, *Anal. Biochem.*, 2004, **324**, 182–270.
5 H. Chandra and S. Srivastava, *Proteomics*, 2010, **10**, 717.
6 P. Cutler, *Proteomics*, 2003, **3**, 3.
7 J. M. Rice, L. J. Stern, E. F. Guignon, D. A. Lawrence and M. A. Lynes, *Biosens. Bioelectron.*, 2012, **31**, 264–269.
8 R. D. Molony, J. M. Rice, J. S. Yuk, V. Shetty, D. Dey, D. A. Lawrence and M. A. Lynes, *Current Protocols in Toxicology*, 2012, 18.16.1.
9 D. J. Cahill, *J. Immunol. Methods*, 2001, **250**, 81.
10 H. Zhu and M. Snyder, *Curr. Opin. Chem. Biol.*, 2003, **7**, 55.
11 D. W. Unfricht, S. L. Colpitts, S. M. Fernandez and M. A. Lynes, *Proteomics*, 2005, **5**, 4432.
12 J. S. Yuk, M. Trnavsky, C. McDonagh and B. D. MacCraith, *Biosens. Bioelectron.*, 2010, **15**, 355.
13 G. Marusov, A. Sweatt, K. Pietrosimone, D. Benson, S. J. Geary, L. K. Silbart, S. Challa, J. Lagoy, D. A. Lawrence and M. A. Lynes, *Environ. Sci. Technol.*, 2012, **46**, 348.
14 V. H. Perez-Luna, S. Yang, E. M. Rabinovich, T. Buranda, L. A. Sklar, P. D. Hampton and G. P. Lopez, *Biosens. Bioelectron.*, 2002, **17**, 71.
15 K. Ray, H. Szmacinski, J. Enderlein and J. R. Lakowicz, *Appl. Phys. Lett.*, 2007, **90**, 251116.
16 M. H. Chowdhury, R. Ray, C. D. Geddes and J. R. Lakwicz, *Chem. Phys. Lett.*, 2008, **452**, 162.
17 E. Matveeva, Z. Gryczynski, J. Malicka, J. Lukomska, S. Makowiec, K. W. Berndt, J. R. Lakwicz and I. Cryczynski, *Anal. Biochem.*, 2005, **344**, 161.
18 M. Trnavsky, J. Enderlein, T. Ruckstuhl, C. McDonagh and B. D. MacCraith, *J. Biomed. Opt.*, 2008, **13**, 054021.
19 J. S. Yuk, C. McDonagh and B. D. MacCraith, *Anal. Bioanal. Chem.*, 2010, **398**, 1947.
20 F. Caruso, K. Niikura, D. N. Furlong and Y. Okahata, *Langmuir*, 1997, **13**, 3422.
21 L. A. Lyon, M. D. Musick and M. J. Natan, *Anal. Chem.*, 1998, **70**, 5177.
22 D. S. Wilson and S. Nock, *Curr. Opin. Chem. Biol.*, 2001, **6**, 81.
23 B. Johnsson, S. Lofas and G. Lindquist, *Anal. Biochem.*, 1991, **198**, 268.
24 *Electromagnetic Theory of Gratings*, ed. R. Petit, Springer-Verlag, Berlin, 1980.
25 U. Schröder, *Surf. Sci.*, 1981, **102**, 118.
26 E. D. Pelik, *Handbook of Optical Constants of Solids I, II, & III*, Academic Press, New York, 1997.
27 T. Akimoto, S. Sasaki, K. Ikebukuro and I. Karube, *Biosens. Bioelectron.*, 2000, **15**, 355.
28 K. B. Lee, S. J. Park, C. A. Mirkin, J. C. Smith and M. Mrksich, *Science*, 2002, **295**, 1702.
29 J. S. Yuk, J. W. Jung, J. Hyun, Y. M. Kim and K. S. Ha, *Sens. Actuators, B*, 2008, **131**, 241.
30 J. D. Swalen, J. G. Gordon, M. R. Philpott, A. Brillante, I. Pockrand and R. Santo, *Am. J. Phys.*, 1980, **48**, 669.
31 B. Liedberg, I. Lundström and E. Stenberg, *Sens. Actuators, B*, 1993, **11**, 63.
32 E. Eulkeith, A. C. Morteani, T. Niedereichholz, T. A. Klar, J. Feldmann, S. A. Levi, F. C. J. M. van Veggel, D. N. Reinhoudt, M. Möller and D. I. Gittins, *Phys. Rev. Lett.*, 2002, **89**, 203002.
33 G. Cnossen, K. E. Drabe and D. A. Wiersma, *J. Chem. Phys.*, 1993, **98**, 5276.
34 H. Kuhn, D. Möbius and H. Bücher, in *Physical Methods of Chemistry*, ed. A. Weissberger and B. W. Rossiter, Wiley Interscience, New York, 1972, Part III B, ch. 7.
35 P. R. Selvin, *Nat. Struct. Mol. Biol.*, 2000, **7**, 730.
36 W. N. Hansen, *J. Opt. Soc. Am.*, 1968, **58**, 380.
37 H. Raether, *Surface plasmons on smooth and rough surfaces and on gratings*, Springer-Verlag, Berlin, 1988.
38 X. Mao, J. Jiang, Y. Luo, G. Shen and R. Yu, *Talanta*, 2007, **73**, 420.
39 J. S. Yuk, B. D. MacCraith and C. McDonagh, *Biosens. Bioelectron.*, 2011, **26**, 3213.

